Physics Letters B 702 (2011) 429–432

Contents lists available at ScienceDirect

Physics Letters B

www.elsevier.com/locate/physletb

The role of spin–orbit potential in nuclear prolate-shape dominance

Satoshi Takahara [a,*], Naoki Onishi [b,c], Yoshifumi R. Shimizu [d], Naoki Tajima [e]

[a] Kyorin University, School of Medicine, Mitaka, Tokyo 181-8611, Japan
[b] University of Tokyo, Japan
[c] University of Yamanashi, Japan
[d] Department of Physics, Graduate School of Science, Kyushu University, Fukuoka 812-8581, Japan
[e] Department of Applied Physics, University of Fukui, 3-9-1 Bunkyo, Fukui 910-8507, Japan

ARTICLE INFO

Article history:
Received 23 May 2011
Received in revised form 27 June 2011
Accepted 11 July 2011
Available online 20 July 2011
Editor: W. Haxton

ABSTRACT

It is confirmed, in terms of the Woods–Saxon–Strutinsky method, that the spin–orbit potential plays a decisive role in the predominance of prolate deformation, which has been a long standing problem in nuclear physics. It is originated from the combined effects of the spin–orbit coupling and the diffused surface of the potential, in agreement with the previous work based on a more schematic Nilsson–Strutinsky method. The degree of prolate-shape dominance exhibits an oscillatory behavior with respect to the strength of spin–orbit potential and, the prolate-shape dominance is realized at the proper strength of the spin–orbit potential together with the standard surface diffuseness; this oscillatory behavior disappears in case of small diffuseness corresponding to ellipsoidal cavity. The calculated energy differences between oblate and prolate minima in this Letter are consistent with those of our extensive self-consistent calculations of the Hartree–Fock + BCS method with the Skyrme interaction.

The discovery of the shell model, i.e., single particle motions in the average potential with spin–orbit term, altered drastically the view of atomic nuclei, which has made it possible to study nuclear structure based on microscopic picture. Soon after the discovery, however, the observed large quadrupole moment [1] turned out to be unexplainable in terms of the spherical shell model, and the concept of nuclear deformation [2,3] together with collective motion was introduced [4]; these concepts have been among the most important ones in the research of nuclear structure. In fact, the evidences of single particle motion in deformed nucleus, i.e., the success of the Nilsson model [5], have been observed, and the concept of nuclear deformation is now commonly accepted. The origin of the nuclear deformation has been studied from a wide variety of view points, and one of simple explanations is the fluctuation of the single particle level density caused by the boundary conditions of the Schrödinger equation at deformed surface of potential [6–8]. Such fluctuation of level density has been interpreted through periodic orbits of quasi-classical theories [9].

From early studies of nuclear deformation, it has been empirically known that most of typical deformed nuclei have prolate rather than oblate shapes; the predominance of prolate deformations is simply called as *prolate-shape dominance* in this Letter. The first attempt to understand the prolate-shape dominance in well-deformed nuclei was made by Lemmer and Weisskopf, changing the strength η of additional potential $H' = \eta r^4$ which steepens the oscillator wall [10]. They had results that the potential with steepened wall override the normal tendency of the harmonic oscillator potential to deform into an oblate shape in the second half of a major shell; i.e., a violation of the particle-hole symmetry. As a limiting case of steep wall, Frisk used a schematic model of ellipsoidal cavities to study the single particle level density through classical periodic orbits, and found prolate deformations favored [11]. It has been, therefore, recognized that the particle-hole symmetry is specific to the harmonic oscillator potential, and the general trend of prolate-shape dominance is brought about by steepening walls. Recently Hamamoto and Mottelson reconfirmed the fact with somewhat different interpretation in terms of the fanning of the low Λ (projection of orbital angular momentum to symmetry axis) orbits [12].

In our extensive calculation of the Hartree–Fock (HF) + BCS method with the Skyrme SIII interaction, the prolate-shape dominance manifests itself, especially, in the region of Mayer–Jensen shell, i.e., $N, Z \geqslant 50$ [13]. This suggests that the spin–orbit potential may play an important role in the prolate-shape dominance. From results obtained by complex procedures of the self-consistent calculations, it is difficult to single out the origin of prolate-shape dominance in relation to energy spectrum of single particle motion.

In principle it is the Hamiltonian of a many-body system, especially the two-body interaction, which determines the shape of

* Corresponding author.
E-mail address: staka@ks.kyorin-u.ac.jp (S. Takahara).

0370-2693
doi:10.1016/j.physletb.2011.07.030

the ground state of the system. As the Strutinsky theory indicates, however, it is always through the one-body level density that the mechanism of this determination works. Thus one can safely assume that various kinds of two-body Hamiltonians give rise to the same ground-state shape if they are reduced to the same one-body Hamiltonian in the mean-field approximation. This is the reason why we prefer to ascribe the origin of the shape to the derived one-body potential rather than to the underlying two-body interaction. For this purpose the Strutinsky theory is indispensable in determining the shape from the one-body potential without specifying the underlying two-body interaction.

For answering the question whether the prolate-shape dominance found in the Skyrme HF+BCS calculation is originated in the radial profile or the spin–orbit potential, one of the authors of this Letter made a preliminary examination by changing the strengths of ℓ^2 (ℓ: magnitude of the orbital angular momentum) term and spin–orbit term in the Nilsson model [14]. The ℓ^2 term is designed to emulate the deviation of the radial profile of the potential from that of the harmonic oscillator, and is included to adjust the single particle energy spectrum to the experiment. It is found that prolate-shape dominance is most remarkable for the standard set of parameters. However, the dominance disappears completely if the strength of the spin–orbit potential is reduced by half. The strength of the ℓ^2 term should be 1.5 times as large as the standard value to reproduce the degree of prolate-shape dominance without the spin–orbit potential. The following significant trends were also observed; with keeping the strength of the ℓ^2 term at the standard value, the degree of prolate-shape dominance oscillates with changing the strength of the spin–orbit potential and becomes most enhanced at the standard value, and the period of the oscillation becomes shorter with enlarging the strength of the ℓ^2 term. Therefore it should be emphasized that the interference between the effects of the ℓ^2 term and the spin–orbit potential is crucial in the actual nuclei. It was also found that pairing correlation enhances both prolate and oblate shape dominances [15].

These results can be ascribed to the fluctuation in the level density which, from the view point of the semiclassical quantization theory, may be originated from a combined effect of three kinds of phases, i.e., one brought about by propagating in medium, one by reflection (Maslov index), and one of geometric origin associated with the Larmor precession (Section 6 in [8]) caused by the spin–orbit potential. A quantitative study is necessary to evaluate the combined effect.

In this Letter, we employ a realistic Woods–Saxon potential to examine this interference. To compare the results of the Woods–Saxon potential with those of the Nilsson potential, we explain briefly parameters characterizing them.

The potential of the Nilsson model is expressed as

$$V(\boldsymbol{r}) = \frac{1}{2}\left(\omega_\perp^2 x^2 + \omega_\perp^2 y^2 + \omega_z^2 z^2\right) + 2\hbar\mathring{\omega}_0 r_t^2 \sqrt{\frac{4\pi}{9}}\epsilon_4 Y_{40}(\hat{\boldsymbol{r}}) + 2 f_{ls}\kappa_N \hbar\mathring{\omega}_0 \boldsymbol{l}_t\cdot\boldsymbol{s} - f_{ll}\kappa_N\mu_N\hbar\mathring{\omega}_0\left(\boldsymbol{l}_t^2 - \langle \boldsymbol{l}_t^2\rangle_N\right), \tag{1}$$

where $\omega_\perp$ and ω_z relate to a deformation parameter ϵ_2 through $\omega_\perp = \mathring{\omega}_0(1+\frac{1}{3}\epsilon_2)$ and $\omega_z = \mathring{\omega}_0(1-\frac{2}{3}\epsilon_2)$ with $\mathring{\omega}_0$ determined by the condition of a volume conservation $\omega_\perp^2\omega_z = \mathring{\omega}_0^3$. We used the standard values given in Table 1 of Ref. [16] for the parameters κ_N and μ_N in each harmonic oscillator shell N. The factors f_{ls} and f_{ll} are introduced to see how prolate-shape dominance changes with these factors when modified from standard values ($f_{ls} = f_{ll} = 1$).

Deformed nuclear shapes (axially symmetric) in Woods–Saxon potential are defined through a surface Σ:

$$R(\theta; R_0, \boldsymbol{\beta}) = R_0 c_v(\boldsymbol{\beta})\left[1 + \sum_\lambda \beta_\lambda Y_{\lambda 0}(\theta)\right], \tag{2}$$

with $\boldsymbol{\beta} \equiv \{\beta_\lambda\}$ and a renormalization factor $c_v(\boldsymbol{\beta})$ to conserve volume. The central part of the potential is given by

$$V_{\rm WS}(\boldsymbol{r}, V_0, \boldsymbol{\beta}) = \frac{V_0}{1 + \exp[\mathrm{dist}_\Sigma(\boldsymbol{r}, \boldsymbol{\beta})/f_a a]} \tag{3}$$

as well as the spin–orbit part

$$V_{\rm SO}(\boldsymbol{r}, \boldsymbol{\beta}) = f_{ls}\lambda\left(\frac{\hbar}{2Mc}\right)^2 \frac{1}{\hbar}\nabla V_{\rm WS}(\boldsymbol{r}, V_0, \boldsymbol{\beta})\cdot(\boldsymbol{\sigma}\times\boldsymbol{p}), \tag{4}$$

where $\mathrm{dist}_\Sigma(\boldsymbol{r}, \boldsymbol{\beta})$ is the (perpendicular) distance between the point $\boldsymbol{r}$ and Σ (taken with the minus sign inside the nucleus), in use of the universal parameter set given in Table 1 of Ćwiok et al. [17]. Similarly, the factors f_a and f_{ls} are introduced to manipulate the potential for studying how prolate-shape dominance depends on those factors, i.e., they control the surface diffuseness and the strength of spin–orbit potential, respectively. It should be noted that the standard value of the diffuseness parameter $a = 0.7$ fm might seem very small compared with the nuclear radius, typically several femtometers, but for large Λ orbits centrifugal potential squeezes wave functions towards the wall to make the effect of diffuseness significant.

In the sense of perturbation, the multipliers f_{ls} for the spin–orbit terms in the two potentials are approximately equivalent. On the other hand, the factors f_a and f_{ll} play quite different roles. For small f_a, potential just inside the surface Σ is deep to increase the binding energy of large ℓ orbitals; therefore, the case with small f_a in the Woods–Saxon model corresponds to the case with large f_{ll} in the Nilsson model. In the limit of small f_a, the radial profile of potential turns to be that of cavity with a finite height, which cannot be rigorously simulated in the Nilsson model.

It is sometimes stated that large diffuseness reduces the spin–orbit splittings of levels. However, they are roughly independent of f_a in the range considered here. The dependence of $V_{\rm SO}$ on f_a through the radial form factor $\nabla V_{\rm WS}$ has only small influences after the integral is done over the radius.

The equilibrium deformation and the ground state energy of each nucleus are determined by the Strutinsky shell correction method [18]. However, the conventional method for realistic finite potential has problems related mainly to the continuum states, see e.g. Ref. [19]. We have recently proposed possible improvements [20] based on the Kruppa prescription [21]. The total energy of a nucleus is assumed to be decomposed into the macroscopic and microscopic parts,

$$E = E_{\rm mac} + E_{\rm mic} \equiv E_{\rm LDM} + (E_{\rm BCS} - \tilde{E}_{\rm BCS}),$$

where $E_{\rm mac} = E_{\rm LDM}$ is the energy of the liquid-drop model, for which the parameters given in Ref. [22] are employed. The energies, $E_{\rm BCS}$ and $\tilde{E}_{\rm BCS}$, are calculated by the BCS treatment for the seniority-type pairing interaction (whose strength is G) with discrete and smoothed level densities, $g(\epsilon)$ and $\tilde{g}(\epsilon)$, respectively,

$$\begin{pmatrix} E_{\rm BCS} \\ \tilde{E}_{\rm BCS}\end{pmatrix} = \int_{-\infty}^{+\infty}\begin{pmatrix} v^2(\epsilon)g(\epsilon) \\ \tilde{v}^2(\epsilon)\tilde{g}(\epsilon)\end{pmatrix}\epsilon\, d\epsilon - \frac{1}{G}\begin{pmatrix}\Delta^2 \\ \tilde{\Delta}^2\end{pmatrix}.$$

As for the smoothed pairing gap, the value $\tilde{\Delta} = 13\,A^{-1/2}$ MeV, is used throughout in this Letter, with which the average trends of the even–odd mass differences are reproduced. More detailed definitions and calculation methods are found in Ref. [20].

We vary the values of multipliers f_{ll}, f_{ls} for the Nilsson potential or f_a, f_{ls} for the Woods–Saxon potential. For each combination (f_{ll}, f_{ls}) or (f_a, f_{ls}), we calculate the total energy curve versus $\epsilon_2(\beta_2)$ ($-0.5 \leqslant \epsilon_2(\beta_2) \leqslant 0.5$ with $\epsilon_4(\beta_4)$ optimized in $-0.16 \leqslant \epsilon_4(\beta_4) \leqslant 0.16$ for each $\epsilon_2(\beta_2)$) for all the even–even nuclei with

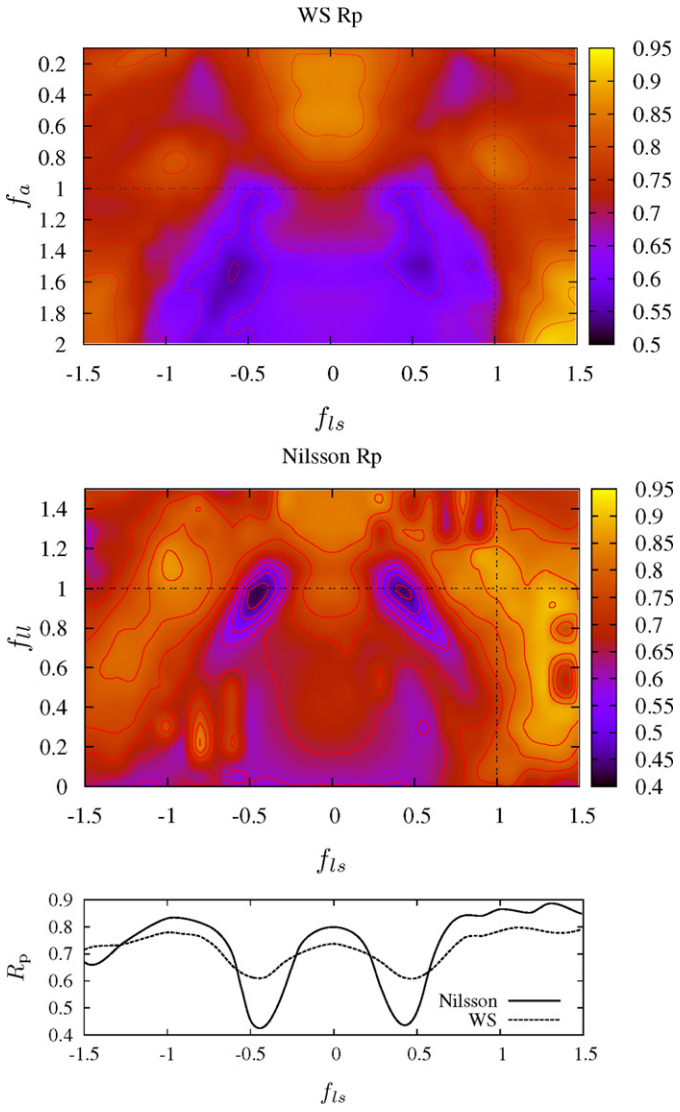

Fig. 1. (Color online.) Proportion of prolate nuclei R_p for Woods–Saxon (top) and Nilsson (middle) potentials and its oscillatory behavior in the line $f_a = 1$ or $f_{ll} = 1$ (bottom).

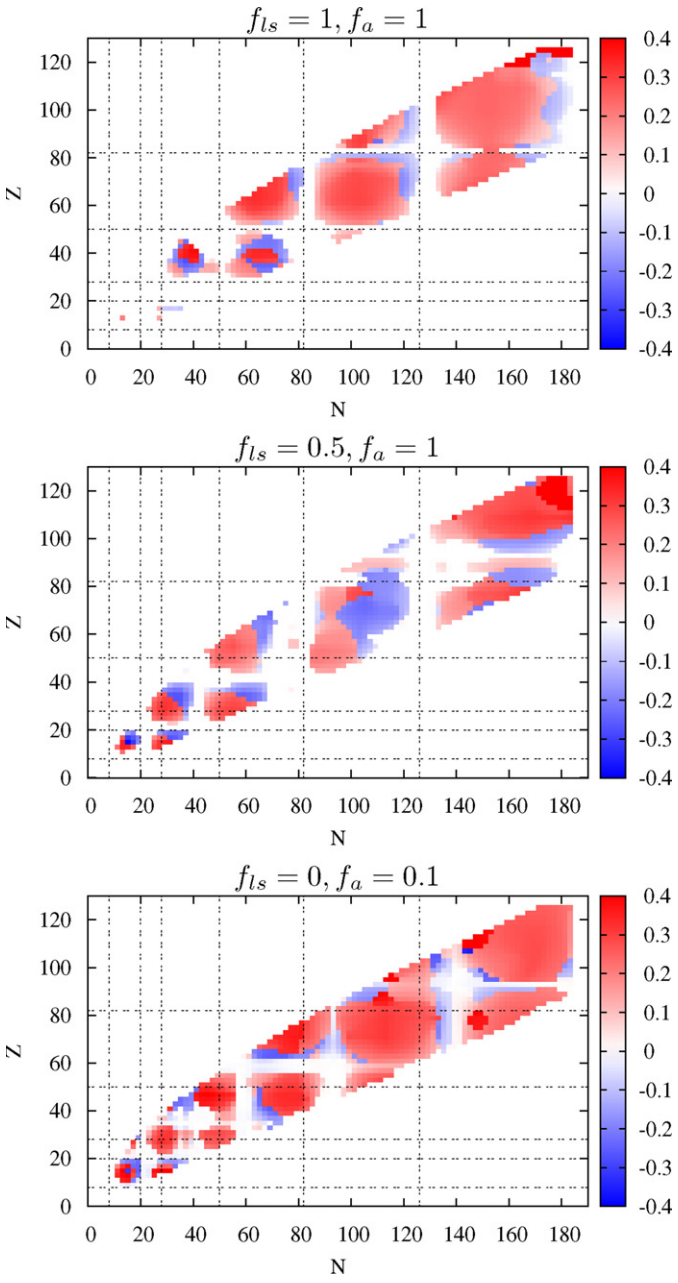

Fig. 2. (Color online.) Location of nuclides with prolate-shape deformation in the periodic charts, for sets of $(f_a, f_{ls}) = (1, 1), (1, 0.5), (0.1, 0)$ at top, middle, and bottom, respectively.

$8 \leqslant Z \leqslant 126$ and $8 \leqslant N \leqslant 184$ and between the proton and neutron drip lines predicted by the Bethe–Weizäcker mass formula.

The way to calculate the proportion of prolate nuclei is the same as in the previous work [14]; the proportion is defined as $R_p = N_p/(N_p + N_o)$, where N_p and N_o are the numbers of nuclei identified as having prolate and oblate deformations, respectively.

The top part of Fig. 1 shows the proportion of prolate nuclei R_p for the Woods–Saxon scheme as a function of the factors f_{ls} vs. f_a ($2 \geqslant f_a \geqslant 0.1, -1.5 \leqslant f_{ls} \leqslant 1.5$). Negative values of f_{ls} do not occur in nuclei but may help one to understand nuclear shapes in the perspective of quantum many-body systems in general. It is compared, in the middle part of Fig. 1, with the same proportion for the Nilsson scheme: As is most clearly seen in the middle part of the figure, the degree of prolate-shape dominance oscillates as changing the strength of the spin–orbit term in both schemes. The significant oscillatory behavior is found along the vertical line of the standard diffuseness value $f_a = 1$, as well as the line of the standard value $f_{ll} = 1$ of the ℓ^2 term. Prolate-shape dominance is most apparent at $f_{ls} = 1$, less apparent at $f_{ls} = -1$, medium at $f_{ls} = 0$, weak at $f_{ls} = \pm 1/2$ in both potentials.

The cooperative effect of the spin–orbit potential and the radial profile is clearly seen also for the realistic Woods–Saxon potential. However, the amplitude of the oscillation is reduced by a factor $\sim \frac{1}{3}$. Consequently, the oblate-shape dominance predicted by the Nilsson model at $f_{ls} \sim \pm 0.5$ is denied by the Woods–Saxon model. The large amplitude obtained with the Nilsson model is likely to be due to an artificial enhancement of the interference between two operators *ls* and *ll* due to their affinity in the sense that both include *l*. Having removed this artifact is one of the significances of our redoing these calculations employing not the Nilsson but the Woods–Saxon potential.

On the other hand for very small diffuseness f_a corresponding to cavity, strong prolate-shape dominance is observed for the Woods–Saxon potential at $f_{ls} = 0$, and the strongly oscillating behavior as a function of f_{ls} disappears. This fact suggests that the

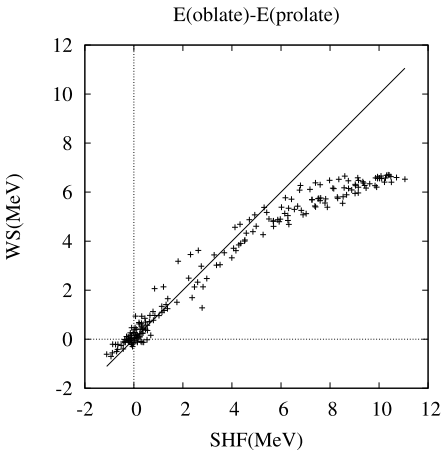

Fig. 3. Comparison of energy differences of oblate from prolate minima, calculated with the Hartree–Fock + BCS (abscissa), and with the Woods–Saxon–Strutinsky methods (ordinate), respectively.

spin–orbit term hardly affect the prolate-shape dominance for potentials with the cavity-like steep radial profile, to which the dominance is solely attributed. The implication is consistent with the statement by Hamamoto and Mottelson [12]. However, for potentials with reasonable radial profiles, the dominance is not enough without the spin–orbit potential. The apparent prolate-shape dominance seen in the case with very small diffuseness does not seem to explain the situation of real nuclei.

Only through looking at the proportion of prolate nuclei, it is difficult to judge which interpretations are more realistic for explaining the nuclear prolate-shape dominance; a glance of nuclear charts of prolate and oblate deformations may be instructive. The top part of Fig. 2 shows the deformation of the ground state on the nuclear chart for standard values of $f_a = f_{ls} = 1$, which is compared with the bottom part depicting that for cavity-like potential without the spin–orbit term. The proportion of prolate nuclei $R_{\rm p}$ is 84% for this cavity-like model ($f_a = 0.1$, $f_{ls} = 0$), while $R_{\rm p}$ is 78% for the standard model ($f_a = f_{ls} = 1$). It is clear that calculations without the spin–orbit potential fail to predict correct locations of spherical nuclei, i.e., the magic numbers. Therefore, all arguments without taking account of spin–orbit potential lack reality in existing nuclei, and therefore have no predictability of deformation for individual nuclides.

The oscillatory behavior, shown at the bottom part of Fig. 1, with respect to the strength of the spin–orbit potential exhibits apparent evidence for interference between two effects coming from the spin–orbit coupling and the surface diffuseness. They work constructively (in phase) at $f_{ls} = 0, \pm 1$ and destructively (out of phase) at $f_{ls} = \pm 0.5$ for prolate-shape dominance. Most of the nuclides predicted as oblate in the case with $f_{ls} = 0.5$, e.g., those with $50 \leqslant Z \leqslant 76$ and $94 \leqslant N \leqslant 116$, in the middle part of Fig. 2 are actually typical prolate deformed nucleus, e.g. ^{166}Dy. In other words the quantitative feature of interference is decisive.

As a concluding remark, let us come back to the starting point of discussion, in which extensive calculations of the HF + BCS method with the Skyrme SIII implies an important role of the spin–orbit potential in the prolate-shape dominance. In Fig. 3, we compare the energy differences of oblate minimum from prolate minimum in the energy surface obtained by the Woods–Saxon–Strutinsky method and the self-consistent mean field theory [13]. This expresses apparent correspondence between two results and implies both calculations predict the same consequences whether a certain nuclide has prolate or oblate deformation; quantitatively, the difference greater than 5 MeV is always enlarged for self-consistent calculations.

While it is impossible to manipulate separately the parameters like f_a and f_{ls} in self-consistent field methods, the Woods–Saxon-Strutinsky method is able to analyze two effects independently. This analysis brings about the discovery of a mechanism in which the interference of combined effects, spin–orbit coupling and spatial profile of potential, results in the predominance of prolate deformation.

References

[1] C.H. Townes, H.M. Foley, W. Low, Phys. Rev. 76 (1949) 1415.
[2] J. Rainwater, Phys. Rev. 79 (1950) 432.
[3] A. Bohr, Phys. Rev. 81 (1951) 134.
[4] D.L. Hill, J.A. Wheeler, Phys. Rev. 89 (1953) 1102.
[5] S.G. Nilsson, Mat. Fys. Medd. Dan. Vid. Selsk. 29 (1955) 16.
[6] B.R. Mottelson, S.G. Nilsson, Mat. Fys. Skr. Dan. Vid. Selsk. 1 (1959) 8.
[7] V.M. Strutinsky, Nucl. Phys. A 95 (1967) 420.
[8] R. Balian, C. Bloch, Ann. Phys. 85 (1974) 514.
[9] V.M. Strutinsky, A.G. Magner, S.R. Ofengenden, T. Døssing, Z. Phys. A 283 (1977) 269.
[10] R.H. Lemmer, V.F. Weisskopf, Nucl. Phys. 25 (1961) 624.
[11] H. Frisk, Nucl. Phys. A 511 (1990) 309.
[12] I. Hamamoto, B.R. Mottelson, Phys. Rev. C 79 (2009) 034317.
[13] N. Tajima, S. Takahara, N. Onishi, Nucl. Phys. A 603 (1996) 23.
[14] N. Tajima, N. Suzuki, Phys. Rev. C 64 (2001) 037301.
[15] N. Tajima, Y.R. Shimizu, N. Suzuki, Prog. Theor. Phys. Suppl. 146 (2002) 628.
[16] T. Bengtsson, I. Ragnarsson, Nucl. Phys. A 436 (1985) 14.
[17] S. Ćwiok, J. Dudek, W. Nazarewicz, J. Skalski, T. Werner, Comput. Phys. Commun. 46 (1987) 379.
[18] V.M. Strutinsky, Sov. J. Nucl. Phys. 3 (1966) 449;
V.M. Strutinsky, Nucl. Phys. A 95 (1967) 420.
[19] W. Nazarewicz, T.R. Werner, J. Dobaczewski, Phys. Rev. C 50 (1994) 2860.
[20] N. Tajima, Y.R. Shimizu, S. Takahara, Phys. Rev. C 82 (2010) 034316.
[21] A.T. Kruppa, Phys. Lett. B 431 (1998) 237.
[22] A.V. Afanasjev, D.B. Fossan, G.J. Lane, I. Ragnarsson, Phys. Rep. 322 (1999) 1.